



A neonatal mouse model for the evaluation of antibodies and vaccines against coxsackievirus A6



Lisheng Yang^{a,1}, Qunying Mao^{b,1}, Shuxuan Li^a, Fan Gao^b, Huan Zhao^a, Yajing Liu^a,
Junkai Wan^a, Xiangzhong Ye^c, Ningshao Xia^a, Tong Cheng^{a,*}, Zhenglun Liang^{b,**}

^a State Key Laboratory of Molecular Vaccinology and Molecular Diagnostics, National Institute of Diagnostics and Vaccine Development in Infectious Diseases, School of Life Sciences, Xiamen University, Xiamen, China

^b National Institutes for Food and Drug Control, Beijing, China

^c Beijing Wantai Biological Pharmacy Enterprise, Beijing, China

ARTICLE INFO

Article history:

Received 18 June 2016

Received in revised form

22 August 2016

Accepted 26 August 2016

Available online 28 August 2016

Keywords:

Coxsackievirus A6

Animal model

Antibody

Vaccine

ABSTRACT

Coxsackievirus A6 (CA6) can induce atypical hand, foot, and mouth disease, which is characterized by severe rash, onychomadesis and a higher rate of infection in adults. Increasing epidemiological data indicated that outbreaks of CA6-associated hand, foot, and mouth disease have markedly increased worldwide in recent years. However, the current body of knowledge on the infection, pathogenic mechanism, and immunogenicity of CA6 is still very limited. In this study, we established the first neonatal mouse model for the evaluation of antibodies and vaccines against CA6. The CA6 strain CA6/141 could infect a one-day-old BALB/c mouse through intraperitoneal and intracerebral routes. The infected mice developed clinical symptoms, such as inactivity, wasting, hind-limb paralysis and even death. Pathological examination indicated that CA6 showed special tropism to skeletal muscles and skin, but not to nervous system or cardiac muscles. Infections with CA6 could induce vesicles in the dermis without a rash in mice, and the CA6 antigen was mainly localized in hair follicles. The strong tropism of CA6 to the skin may be related to its severe clinical features in infants. This mouse model was further applied to evaluate the efficacy of a therapeutic antibody and an experimental vaccine against CA6. A potential mAb 1D5 could fully protect mice from a lethal CA6 infection and also showed good therapeutic effects in the CA6-infected mice. In addition, an inactivated CA6 vaccine was evaluated through maternal immunization and showed 100% protection of neonatal mice from lethal CA6 challenge. Collectively, these results indicate that this infection model will be a useful tool in future studies on vaccines and antiviral reagents against CA6.

© 2016 Elsevier B.V. All rights reserved.

1. Introduction

Hand, foot, and mouth disease (HFMD) is a highly contagious disease that affects infants and children around the world, particularly in the Asia-Pacific region (Lei et al., 2015). Enterovirus 71 (EV71) and coxsackievirus A16 (CA16) have been the predominant causes of HFMD in the last ten years (Lei et al., 2015; Mao et al., 2014; Xing et al., 2014). However, increasing epidemiological data indicates that the number of HFMD epidemics associated with

coxsackievirus A6 (CA6) has markedly increased worldwide in recent years (Bian et al., 2015; Feder et al., 2014; Mirand et al., 2012; Montes et al., 2013). Additionally, CA6 has even replaced EV71 and CA16 as the predominant pathogen in some HFMD outbreaks in Europe (Cabrerizo et al., 2014; Kobayashi et al., 2013), Asia (Gopalkrishna et al., 2012; Han et al., 2014; Miyamoto et al., 2014; Wu et al., 2010) and North America (Centers for Disease Control and Prevention, 2012; Fonseca et al., 2014; Klein and Chong, 2015).

CA6 belongs to the human enterovirus species A within the *Picornaviridae* family. CA6-associated HFMD is characterized by widespread vesicubullous eruption (Stewart et al., 2013), onychomadesis (Osterback et al., 2009; Wei et al., 2011), herpangina (Mirand et al., 2012), and higher rate of infection in adults (Downing et al., 2014), which is different from traditional HFMD caused by EV71 and CA16. Because of the outbreaks of CA6 and the

* Corresponding author.

** Corresponding author.

E-mail addresses: tcheng@xmu.edu.cn (T. Cheng), lzhenglun@126.com (Z. Liang).

¹ These authors contributed equally to this work.

severity of its clinical manifestations, CA6 has recently attracted the attention of researchers around the world. However, studies of CA6 have just begun, and the current body of knowledge on the infection, pathogenic mechanism, and immunogenicity of CA6 is still very limited.

The development of an animal model is indispensable in studying the pathogenic mechanism and evaluating the efficacy of vaccines or antiviral reagents. Animal models of EV71 and CA16 have been constructed based on various types of animals, such as neonatal mice, adult immune-deficient mice, transgenic mice and non-human primates (Liu et al., 2014; Wang and Yu, 2014). These animal models have greatly facilitated the process of vaccine development and the understanding of the pathogenesis of HFMD. Specifically, small animal models have been widely used in assessing the efficacy of experimental vaccines at early stages. The increasing number of CA6 epidemics has increased the need for animal models of CA6. However, no neonatal mouse model has been established to evaluate the efficacy of vaccines or therapeutic antibodies against CA6.

In a previous study, we reported that an isolated CA6 strain CA6/141 could grow in RD cells with high titers and showed high virulence in one-day-old suckling mice (Yang et al., 2015). In this study, a neonatal mouse model was further established based on this CA6 strain, and the pathogenic characteristics of CA6 in mice were analyzed. This mouse model was also applied to evaluate the efficacy of a therapeutic antibody and an experimental vaccine against CA6.

2. Materials and methods

2.1. Cells, virus and monoclonal antibodies

Human rhabdomyosarcoma (RD) cells were maintained in MEM as previously described (Yang et al., 2014). The CA6 strain CA6/141 (GenBank: KR706309.1), a gift from National Taiwan University, was propagated in RD cells and stored at -80°C in our laboratory (Yang et al., 2015). The 50% tissue culture infectious dose (TCID_{50}) of CA6/141 was determined by the method described by Reed and Muench (Reed and Muench, 1938). Anti-CA6 monoclonal antibodies (mAbs) were screened and produced using the methods previously described (Ye et al., 2016). Live CA6/141 emulsified in Freund's adjuvant was used as an immunogen. All mAbs were stored at -20°C in our laboratory.

2.2. Mouse infection

The specific pathogen-free (SPF) mice used in this study included inbred BALB/c, C57BL/6 mice and outbred Kunming (KM), ICR, NIH mice (Slac Laboratory Animal Co., Ltd., Shanghai, China). The use of the mice was approved by the Institutional Animal Care and Use Committee at Xiamen University. All institutional guidelines for animal care and use were strictly followed throughout the experiments.

For the selection of sensitive mouse strains for the experiments, one-day-old mice of different strains were intraperitoneally (i.p.) challenged with 100 μL of CA6/141 (10^5 TCID_{50} per mouse). For the dose-dependent experiments, one-day-old BALB/c mice were i.p. challenged with 100 μL of 10-fold serially diluted CA6/141 (10^2 – 10^6 TCID_{50} per mouse). In the route-dependent study, one-day-old BALB/c mice were challenged with CA6/141 (10^5 TCID_{50} per mouse) via i.p., intracerebral (i.c.), or intragastric (i.g.) routes. For i.g. routes, a 24-gauge feeding tube was used to inoculate the mice after 6 h of fasting. For the age-dependent experiments, mice were selected at 1, 3, 5, 7, 14, and 21 days of age and i.p. challenged with 10^5 TCID_{50} of CA6/141. The control mice were mock-infected with

100 μL of PBS via the same route.

Each group contained 8–10 mice. All mice were monitored daily for body weight, clinical illness and death until 20 days post-infection (dpi). The grade of clinical disease was scored as follows: 0, healthy; 1, lethargy and inactivity; 2, wasting; 3, limb weakness; 4, hind-limb paralysis; and 5, morbidity and death.

2.3. Histopathological examination and immunohistochemical staining (IHC)

The experiments were performed as previously described (Li et al., 2014). Briefly, the mice with clinical disease (grades 4 to 5) and the control mice (grade 0) were euthanized with carbon dioxide and subjected to histopathologic and immunohistochemical examination. Various organ or tissue samples (blood, brain, spinal cord, heart, lung, liver, spleen, kidney, intestines, and limb muscles) were isolated and fixed by immersion in 4% formalin for at least 72 h at room temperature. After fixation, tissues were dehydrated in ethanol gradients, embedded in paraffin and sliced into 4-mm-thick array sections. For histopathologic examination, tissue sections were stained with hematoxylin and eosin. IHC staining of the tissue sections was performed using an Ultrasensitive TM S-P kit (Fuzhou Maixin Biotechnology Development Co., Ltd., Fuzhou, China) and DAB detection kit (Streptavidin-Biotin; Fuzhou Maixin Biotechnology Development Co., Ltd., Fuzhou, China) according to the manufacturer's instructions. Anti-CA6 mAb 1D5 was used as the primary antibody (1 mg/mL, 1:500 dilution).

2.4. Tissue sampling and qRT-PCR

Groups of one-day-old BALB/c mice were i.p. challenged with 100 μL of CA6/141 (10^5 TCID_{50} per mouse) or 100 μL of PBS. Organ or tissue samples were collected at 6, 24, 48, 72, and 96 h post-infection (4 mice per time point): blood samples were harvested by heart puncture, and tissues from the brain, spinal cord, heart, lung, liver, spleen, kidney, intestines, and limb muscles were isolated, weighed, and stored at -80°C . The mouse tissues were homogenized in 200 μL of PBS by a high-throughput tissue grinder (Scientz-192, Scientz, Ningbo, China). Viral RNA was extracted from blood samples and tissue homogenates using a viral DNA/RNA purification kit (GenMag Bio, Beijing, China) according to the manufacturer's instructions. For quantification, RT-PCR analysis was performed with a one-step RT-PCR Kit (GenMag Bio, Beijing, China) following the manufacturer's protocol with the primers F-EV (5'-GCCCTGAATGCGGCTAATCCTAA-3'), R-EV (5'-CGGACACCCAAAGTAGTCGGTTCC-3') and the probe (5'-CCGATACGACGCACCACCCCTGGATTGA-BHQ) in the ABI 7500 system. RT-PCR reactions were carried out as follows: 15 min at 42°C and 15 min at 95°C , followed by 40 cycles of 95°C for 15 s and 55°C for 55 s. The fragments amplified by the primers F-EV and R-EV were inserted into pMD18-T plasmid, resulting in the plasmid pMD18-T-EV, which was used to calculate the absolute copies of CA6.

2.5. Evaluation of antibody and maternal immunization experiments

To evaluate the effect of a mAb on the prevention of CA6 infection *in vivo*, one-day-old mice were i.p. inoculated with mAb 1D5 at doses of 5 μg , 15 μg , or 30 μg per body weight (g). Control mice were treated with PBS via the same route. Twelve hours later, all mice were i.p. inoculated with 10^5 TCID_{50} of CA6/141.

For antibody treatment experiments, one-day-old mice were first i.p. inoculated with 10^5 TCID_{50} of CA6. Twenty-four hours later, mAb 1D5 was i.p. inoculated at doses of 0.25 μg , 5 μg , 15 μg , 30 μg ,

or 60 µg per body weight (g). The mice in the control group were treated with PBS via the same route.

In the maternal immunization experiment, CA6/141 was inactivated with 0.1% formaldehyde at 37 °C for 24 h and formulated with an aluminum phosphate adjuvant. Six-week-old female BALB/c mice were immunized by i.p. inoculation with 0.5 mL of the inactivated CA6 (10^6 TCID₅₀ per mouse) and received the same dose of booster injections after 2 weeks. The mice immunized with MEM were used as controls. The immunized animals were bled at 0, 2, 4, 6, and 8 weeks for the serological tests, and the serum was collected and stored at -20 °C. The mice were allowed to mate after the second booster immunization. The neonatal mice were i.p. challenged with 10^5 TCID₅₀ per mouse of CA6 within 24 h after birth. All mice were monitored daily for body weight, clinical illness and death until 20 dpi.

2.6. Statistical analysis

All statistical analyses were performed with GraphPad Prism software (version 5.01) for Windows. Survival curves were compared by the log-rank (Mantel-Cox) test. The 50% lethal dose (LD₅₀) and the concentration required for 50% of maximal effect (EC₅₀) were determined by the methods described by Reed and Muench (Reed and Muench, 1938). A P value < 0.05 was considered statistically significant.

3. Results

3.1. Selection of mouse strains

To determine which mouse strain was susceptible to infection with CA6, 5 mouse strains were chosen: inbred mouse strains BALB/c and C57BL/6 and outbred mouse strains KM, ICR, and NIH. Groups of one-day-old mice (5–8 mice per group) were i.p. challenged with 100 µL of CA6/141 (approximately 10^5 TCID₅₀ per mouse). The inbred BALB/c mice and the outbred mouse strains KM, ICR and NIH developed clinical symptoms, such as inactivity, wasting, and hind-limb paralysis, and 100% died within 5 dpi, indicating that these strains were very sensitive to CA6 infection. In contrast, 50% of the C57BL/6 mice were still alive 20 dpi, and this mouse strain seemed to be less sensitive to CA6 infection (Table 1). Compared with the outbred mice strains, the inbred BALB/c mice had an identical genetic background with more stable results; therefore, the BALB/c mice were selected for further studies.

3.2. BALB/c mice are susceptible to CA6 infection via i.p. and i.c. routes

To select a suitable inoculation route, one-day-old BALB/c mice were infected via i.p., i.c. or i.g. routes with 10^5 TCID₅₀ of CA6/141. As shown in Fig. 1, both mice inoculated via the i.c. and i.p. routes became sick at 3 dpi, which resulted in a 100% mortality rate. However, the mortality rate of mice i.g. infected with CA6 was only 12.5%, which differed greatly from the i.p. and i.c. routes. These results indicated that both the i.p. and i.c. routes were suitable for

Table 1
Selection of mouse strains sensitive to infection with CA6.

Mouse line	Mouse strain	Mortality
Inbred mouse	BALB/c	5/5
	C57BL/6	4/8
Outbred mouse	KM	6/6
	ICR	6/6
	NIH	5/5

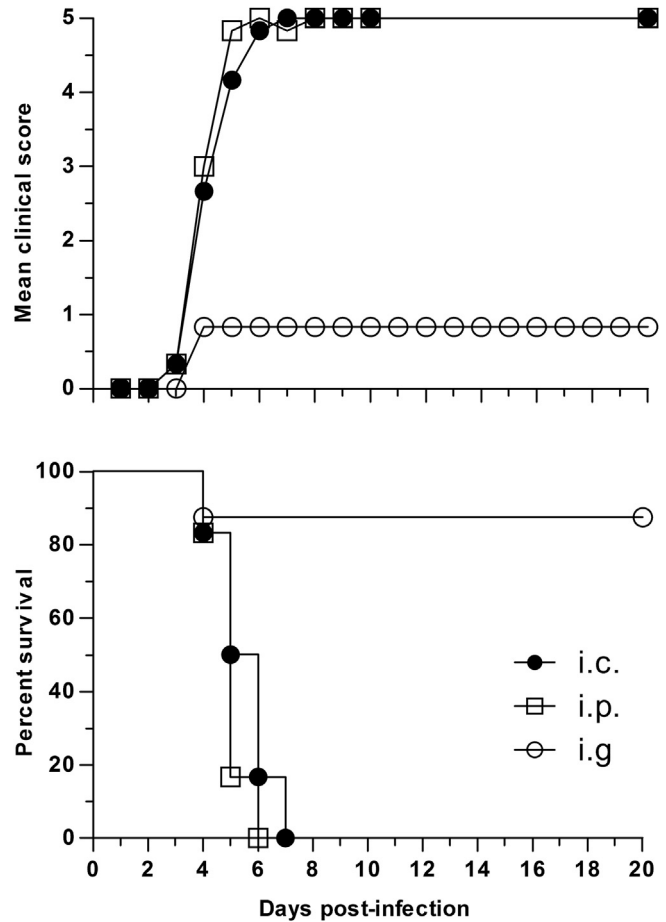


Fig. 1. Selection of a suitable inoculation route. One-day-old BALB/c mice (8–10 mice per group) were challenged with CA6/141 (10^5 TCID₅₀ per mouse) via intraperitoneal (i.p.), intracerebral (i.c.), or intragastric (i.g.) routes. All mice were monitored daily for body weight, clinical illness, and death until 20 days post-infection.

CA6 infection. For convenience, the i.p. route was used as the standard route of infection of CA6 in the following experiments.

3.3. BALB/c mice infected with CA6 developed age-related disease and mortality

To compare the susceptibility of mice of different ages to CA6, groups of the BALB/c mice at 1, 3, 7, 14, and 21 days of age were i.p. inoculated with CA6/141 (10^5 TCID₅₀ per mouse). The results showed that only the one-day-old mice became sick, and 100% died within 4 dpi. In contrast, no clinical symptoms were observed in 3-day-old or older mice within 20 dpi (Fig. 2). However, when the infectious dose was increased to 10^6 TCID₅₀ per mouse, the 3-day-old mice became sick at 4 dpi, and all of these mice died within 7 dpi. These results suggested that one-day-old mice were the most susceptible to CA6; however, the mice older than one day were also susceptible to CA6 infection, but a much greater infectious dose was needed. Therefore, BALB/c mice at one day of age were selected as the animal model in this study.

3.4. Infection of BALB/c mice with CA6 presented dose-dependent disease and mortality

To determine the suitable infectious dose of CA6 and LD₅₀, one day-old BALB/c mice were i.p. inoculated with 10-fold serially

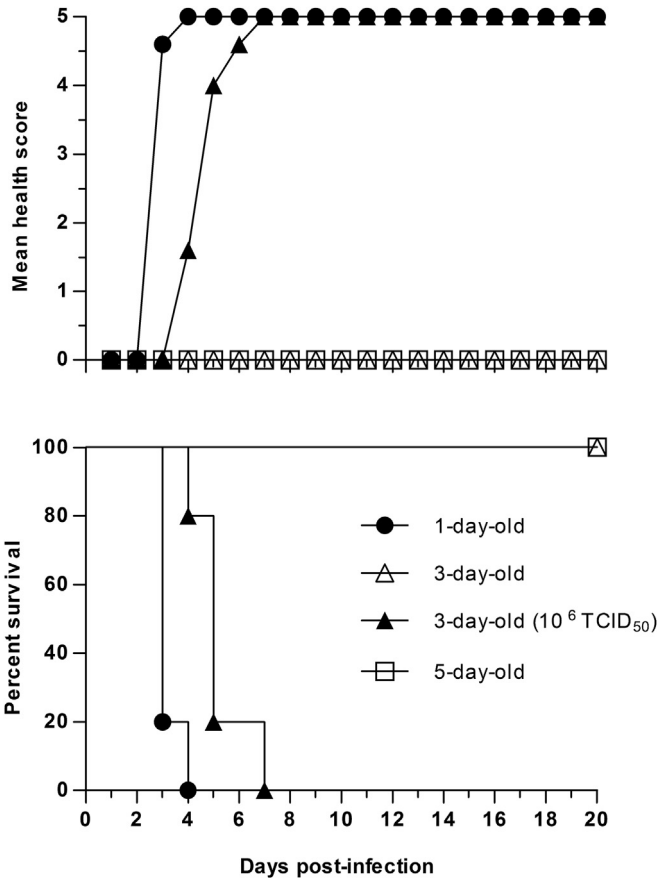


Fig. 2. BALB/c mice infected with CA6 developed age-related disease and mortality. BALB/c mice at 1, 3, 7, 14, and 21 days of age (8–10 mice per group) were i.p. inoculated with CA6/141 (10^5 or 10^6 TCID₅₀ per mouse). All mice were monitored daily for body weight, clinical illness and death until 20 days post-infection. Mice at 7, 14, and 21 days of age did not develop any significant symptoms, and the related data were excluded and are not shown.

diluted CA6 (10^2 to 10^6 TCID₅₀ per mouse). The results showed that mice infected with doses of 10^6 and 10^5 TCID₅₀ quickly died within 4 dpi (Fig. 3). When the infectious doses were reduced to 10^4 , 10^3 , and 10^2 TCID₅₀ per mouse, the mice became sick at 4, 5, and 6 dpi, respectively, and the ultimate mortality rates fell from 90% to 10%. In contrast, the control mice treated with PBS were healthy throughout the experiment. These results indicated that there was a significant dose-response effect between the infectious dose of

CA6 and the mortality rate of the mice. The LD₅₀ of CA6/141 was 1.33×10^3 TCID₅₀ per mouse. Finally, the standard infectious dose of CA6/141 was determined as 10^5 TCID₅₀ per mouse (approximately 75 LD₅₀).

3.5. Pathology of CA6-infected mice

CA6-associated HFMD was characterized by a severe rash and onychomadesis, which was different from the symptoms induced by EV71 or CA16. It indicated that the tissue tropism of CA6 was somewhat different from that of EV71 or CA16. To characterize the pathogenic mechanism of CA6 in mice, histopathological examinations were performed on the CA6-infected mice that developed clinical symptoms (grade levels 4–5, Fig. 4A). As shown in Fig. 4B, a massive spread of the CA6 antigen was detected in the skeletal muscles of the hind-limb and spine. The H&E staining results showed that these skeletal muscles exhibited severe necrotizing myositis with inflammatory infiltration. In addition, many vesicles were formed in the dermis, and positive signals were observed in the hair follicles. However, no skin rashes occurred in mice. These results indicated that CA6 had a strong tropism to the skeletal muscles and skin. In contrast to EV71 or CA16, CA6 did not show significant tropism to the nervous or cardiac tissues. The other organs of the infected mice, such as the heart, liver, intestine, kidney, spleen, and lungs, were also examined, but no significant histological changes or viral antigens were observed (data not shown).

3.6. Tissue viral loads in CA6-infected mice

To further understand the dynamic of viral loads in different organs or tissues, the viral loads in the blood, heart, brain, liver, intestine, kidney, spleen, lungs, and limb muscles of the CA6-infected mice were determined by real-time RT-PCR at different time points post-infection. As shown in Fig. 5, CA6 could be detected in most organs with relatively low viral copies (10 to 10^3 copies/mg) at 6 h post-infection, especially the viral loads in the brain and blood (<10 copies/mg). As time went on, CA6 titers in most of the organs increased, but the viral loads in the spleen and liver increased more rapidly than the other tissues in the first 24 h post-infection and remained stable at high levels before 72 h post infection, indicating that the spleen and liver would likely be the target organs of CA6 at the early stage of infection. However, the viral load in the limb muscles increased most rapidly in the time period between 24 h and 72 h post-infection, and the highest viral titer in the limb muscles reached up to 1×10^7 copies/mg, suggesting that the limb muscle was the main site of CA6 replication. While the mice exhibited clinical symptoms at grade 4 for an

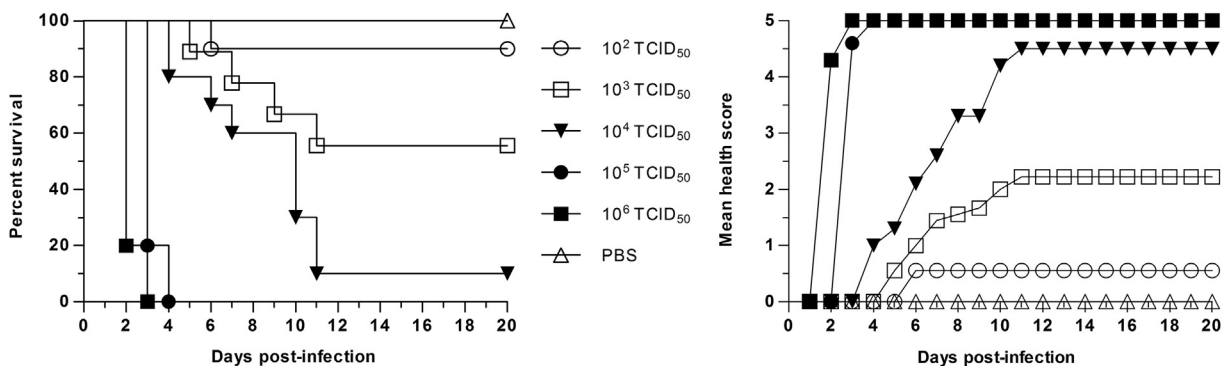


Fig. 3. Infection of BALB/c mice with CA6 resulted in dose-dependent disease and mortality. One-day-old BALB/c mice (8–10 mice per group) were i.p. inoculated with 10-fold serially diluted CA6 (10^2 to 10^6 TCID₅₀ per mouse) or PBS. All mice were monitored daily for body weight, clinical illness and death until 20 days post-infection.

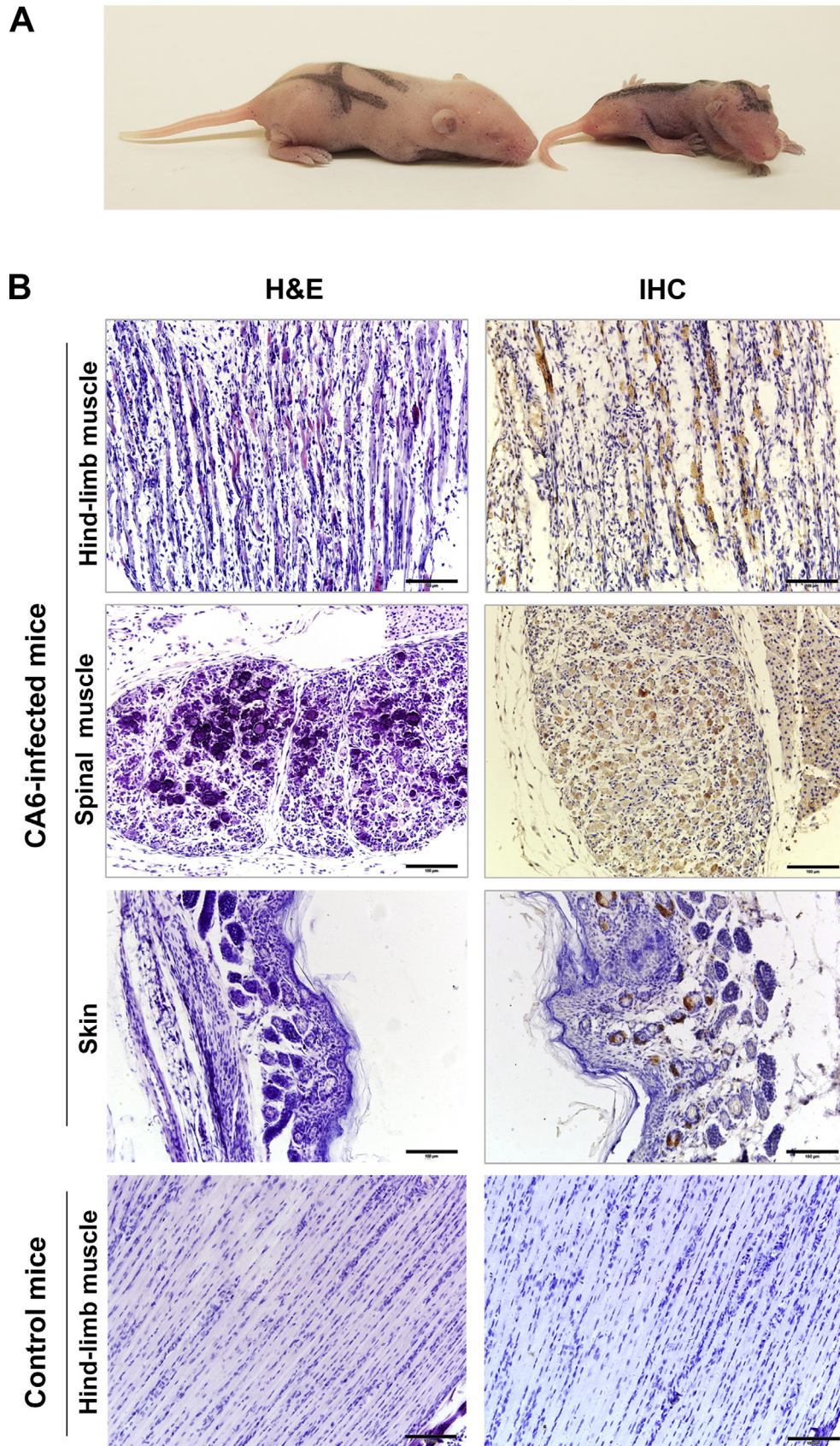


Fig. 4. Pathology of CA6-infected mice. (A) A representative picture of clinical symptoms induced by CA6 in mice. The CA6-infected mice (the left side) showed wasting hind limb paralysis. The mice treated with PBS were used as control (the right side). (B) Histopathological examination (H&E) and immunohistochemical staining (IHC) were performed on the CA6-infected mice that developed clinical symptoms (grade levels 4–5). The anti-CA6 mAb 1D5 was used as the primary antibody (1 mg/mL, 1:500 dilution). Scale bars, 100 μ m.

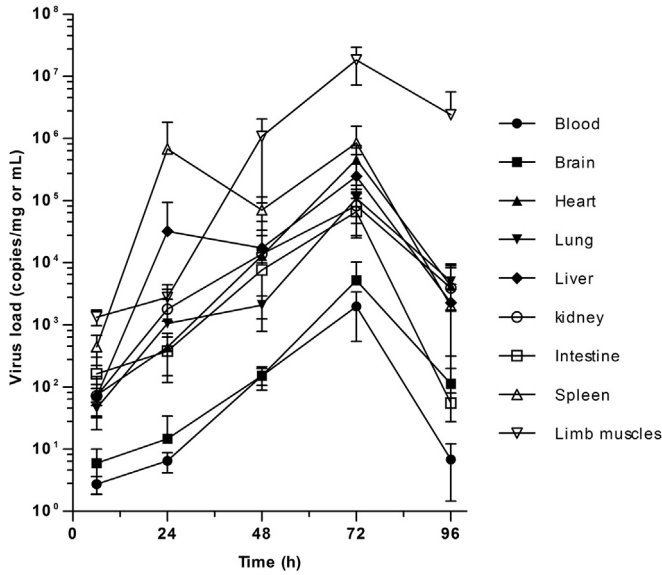


Fig. 5. Tissue viral loads in CA6-infected mice. One-day-old BALB/c mice were first i.p. inoculated with 100 μ L of CA6/141 (10^5 TCID₅₀ per mouse). Tissue samples were collected at 6, 24, 48, 72, and 96 h post-infection. The viral loads in the blood, brain, heart, lungs, liver, kidney, intestine, spleen, and lower limb muscles of the CA6-infected mice were determined by real-time RT-PCR. The error bars show the standard deviations between replicates (n = 4).

average of 72 h post-infection, the viral loads in most of organs or tissues peaked, suggesting that CA6 had infected the entire body. Most of the CA6-infected mice died at 96 h post-infection, and only

approximately 20% of the mice survived. Only the surviving mice were sampled. As shown in Fig. 5, the viral loads in the organs or tissues of the surviving mice were lower than those of mice at 72 h post-infection.

3.7. Application of the mouse model in the evaluation of a therapeutic mAb

A neutralizing mAb 1D5 was produced in our laboratory, and it could neutralize CA6 *in vitro* (neutralizing titer, 1:512) and specifically recognize the CA6 antigen (Yang et al., 2015). To evaluate the therapeutic effect of mAb 1D5 *in vivo*, one-day-old mice were first i.p. challenged with CA6 and then i.p. inoculated with a single dose of mAb 1D5 at concentrations of 0.25 μ g, 5 μ g, 15 μ g, 30 μ g, or 60 μ g per body weight (g) 24 h later. As shown in Fig. 6A, the mice treated with 0.25 μ g/g mAb 1D5 developed clinical symptoms at 2 dpi and 100% died at 7 dpi. In contrast, 78% of the mice treated with 5 μ g/g of mAb 1D5 survived. When raising the concentration of mAb 1D5 to 15 μ g/g or 30 μ g/g, the survival rate of mice did not change but showed a delayed onset (Fig. 6A). However, when the concentration of mAb 1D5 was increased to 60 μ g/g, 100% of mice survived, and no significant clinical symptoms were observed within 20 dpi. The EC₅₀ of mAb 1D5 was approximately 3 μ g/g.

3.8. The neutralizing mAb 1D5 could prevent CA6 from infecting neonatal mice

In another experiment, neonatal mice were passively immunized with mAb 1D5 to evaluate its effect on protection against CA6 infection. 100 μ L of mAb 1D5 with different concentrations were i.p.

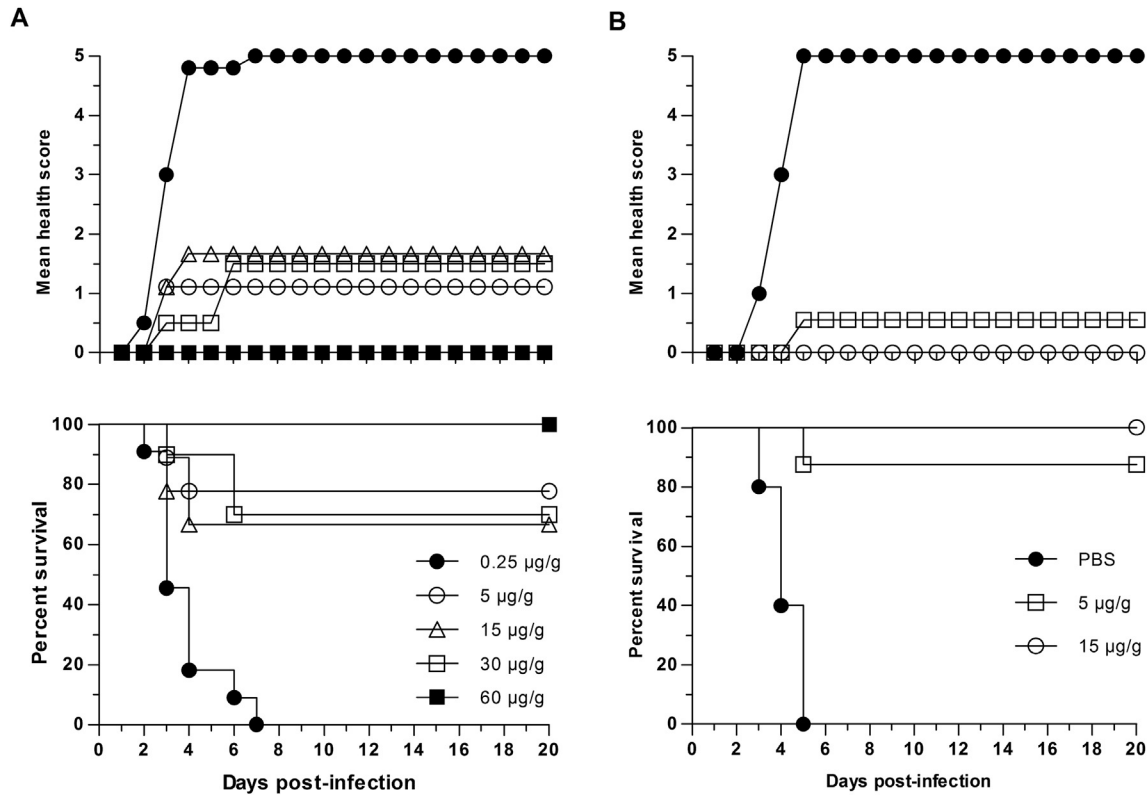


Fig. 6. Evaluation of the protective effect and therapeutic effect of anti-CA16 mAb 1D5 *in vivo*. (A) For antibody treatment experiments, one-day-old mice were first i.p. infected with 10^5 TCID₅₀ of CA6. At 24 h post-infection, mAb 1D5 was i.p. injected at a concentration of 0.25 μ g, 5 μ g, 15 μ g, 30 μ g, or 60 μ g per body weight (g). Each group contained 8–10 mice. (B) To evaluate the effect of the mAb in preventing CA6 infection *in vivo*, one-day-old mice were i.p. administered with mAb 1D5 at doses of 5 μ g, 15 μ g, or 30 μ g per body weight (g). Control mice were treated with PBS by the same route. Approximately 12 h later, all mice were i.p. infected with 10^5 TCID₅₀ CA6/141. All mice were monitored daily for body weight, clinical illness and death until 20 days post-infection.

inoculated to one-day-old mice 12 h prior to a lethal challenge of CA6. The control group was i.p. inoculated with PBS instead of mAb 1D5. As shown in Fig. 6B, all of the mice that were passively immunized with mAb 1D5 at doses of 15 $\mu\text{g/g}$ or 30 $\mu\text{g/g}$ survived, and no significant clinical symptoms were observed throughout the experiment. When the dose of mAb 1D5 was reduced to 5 $\mu\text{g/g}$, 90% of the mice were still protected. Conversely, the control mice started to display severe clinical symptoms at 3 dpi, and all died at 5 dpi (Fig. 6B). Thus, to provide 100% protection against CA6 infection, approximately 15 $\mu\text{g/g}$ or even higher doses of mAb 1D5 should be passively administered to neonatal mice.

3.9. Maternal antibodies protected neonatal mice from CA6 infection

Maternal antibodies can be transferred to infants through the placenta and breastfeeding and protect young infants from infectious diseases. In this section, the protection efficacy of an experimental formalin-inactivated CA6 was evaluated through maternal immunization. Six-week-old female mice were first immunized with the formalin-inactivated CA6/141 and allowed to mate after the last immunization. The mice immunized with MEM were used as controls. The neonatal mice were challenged with 10^5 TCID₅₀ of CA6/141 on the day of birth. As shown in Fig. 7, the neonatal mice

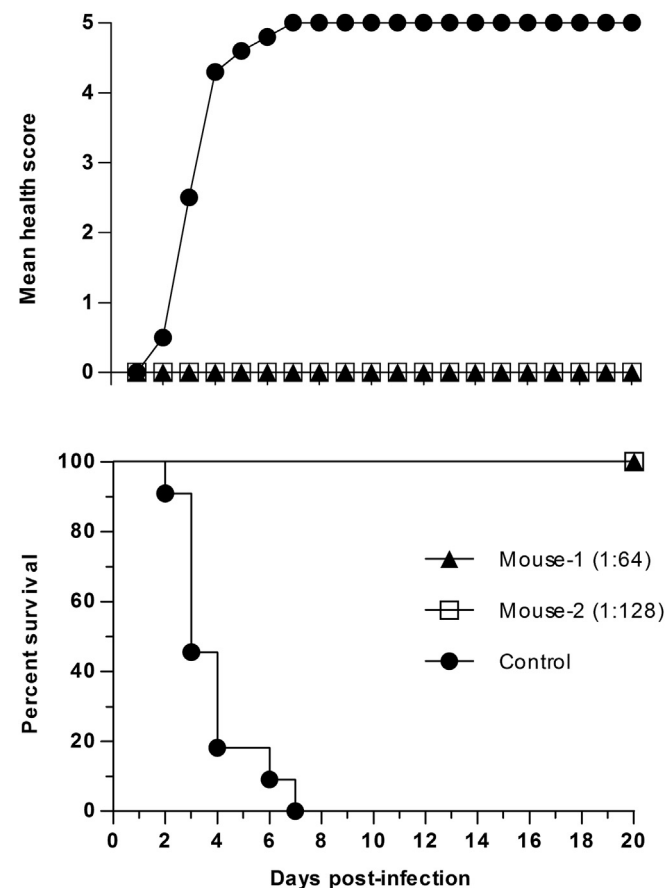


Fig. 7. Application of the neonatal model in evaluating a vaccine against CA6. Six-week-old female BALB/c mice were immunized by i.p. inoculation with 0.5 mL of the formaldehyde-inactivated CA6 (10^6 TCID₅₀ per mouse) and received the same dose of booster injection after 2 weeks. The mice were allowed to mate after the second booster immunization. The mice immunized with MEM were used as controls. The neonatal mice were i.p. challenged with 10^5 TCID₅₀ per mouse of CA6 within 24 h after birth. All mice were monitored daily for body weight, clinical illness and death until 20 dpi.

birthed by mothers with a serum neutralizing titer of 1:64 or 1:128 all survived with no significant clinical symptoms within 20 dpi. In contrast, the neonatal mice in the control group started to become sick at 2 dpi, and all died at 7 dpi.

4. Discussion

The evaluation of the efficacy of experimental vaccines and antiviral reagents depends on a valid animal model. Thanks to the animal models of EV71 and CA16, vaccines against these two viruses progressed well, and EV71 vaccines were recently approved by the China Food and Drug Administration (CFDA) (Mao et al., 2016). Because the neonatal mouse model is sensitive, stable, easily acquired and low-cost, it has been widely used in study of HFMD-related enteroviruses (Liu et al., 2014; Wang and Yu, 2014). The outbreaks of CA6-associated HFMD boosted the demand for vaccines against CA6 and related animal models. CA6 is typically isolated and cultured in neonatal mice, while it is difficult to isolate or culture with cells susceptible to most enteroviruses (Bian et al., 2015; Liu et al., 2015; Schmidt et al., 1975). In a previous study, we reported that an isolated CA6 strain CA6/141 could grow in RD cells with high titers and showed high virulence in one-day-old neonatal mice (Yang et al., 2015). The CA6/141 strain belongs to lineage E, which is the predominant strain associated with HFMD worldwide (Bian et al., 2015). The high virulence of the CA6/141 strain makes it possible for us to develop a potential animal model of CA6 infection.

The characteristics of the infection of neonatal mice with CA6 were first reported in 1951 (Gifford and Dalldorf, 1951). Unlike EV71 and CA16 (Mao et al., 2012; Wang and Yu, 2014), CA6 showed weak tropism to nervous system or cardiac muscles in the mice. However, our results indicated that CA6 had significant tropism to skeletal muscles and skin. Infections with CA6 could induce vesicles in the dermis without a rash in the mice, and the CA6 antigen was localized mainly in hair follicles. In contrast, vesicle formation in the epidermis and upper dermis was also observed in CA6-infected HFMD patients, but the CA6 antigen was mainly detected in keratinocytes (Muehlenbachs et al., 2015; Seki et al., 2014). This may explain why skin lesions are commonly observed in humans but are seldom observed in mouse models. The strong tropism of CA6 to the skin may be related to its severe clinical features in infants.

In this study, the neonatal mouse model was first applied to evaluate a therapeutic anti-CA6 mAb and an experimental CA6 vaccine. Antibodies have been used for the prevention and treatment of various types of infectious diseases (Keller and Stiehm, 2000). Neonates and immunodeficient adults are particularly susceptible to infections with CA6 and are liable to develop severe clinical symptoms (Bian et al., 2015; Christoffers et al., 2016; Reina et al., 2014). Passive immunization with anti-CA6 neutralizing antibodies might provide protection in such populations. A neutralizing mAb named 1D5 was produced in our laboratory, and it showed high neutralizing capacity against CA6 *in vitro*. Passive immunization with mAb 1D5 with a dose of 15 $\mu\text{g/g}$ could protect 100% of neonatal mice from lethal CA6 challenge. It also showed a good therapeutic effect in the CA6-infected mice. These data indicated that the mAb 1D5 is a potential therapeutic mAb against CA6 for further humanization.

Vaccine immunization is believed to be the most effective tool to control the HFMD epidemic. However, experimental EV71 and CA16 vaccines could not induce cross-protection against infection with CA6 (Liu et al., 2014). The development of vaccines against CA6 will be the focus of future research. Indeed, several groups have begun to assess the feasibility of CA6 vaccines (Caine et al., 2015; Liu et al., 2015, 2016). Caine et al. (2015) recently established a mouse

model based on immunodeficient AG129 mice using a mouse-adapted CA6 strain. The passive transfer of immune serum, which was raised by a trivalent HFMD vaccine against EV71, CA16 and CA6, could protect 3-week-old mice from lethal CA6 challenge. However, the pathogenic characteristics of the mouse-adapted CA6 strain in mice were not fully explored. In this study, we evaluated the efficacy of an inactivated CA6 vaccine through maternal immunization, which has been widely used for the evaluation of EV71 or CA16 vaccines (Mao et al., 2012).

In conclusion, we established a neonatal mouse model using a non-mouse-adapted CA6 strain and demonstrated that CA6 had strong tropism to the skin and skeletal muscle, which may be related to its severe clinical features in humans. The neonatal mouse model was successfully applied to evaluate a therapeutic mAb and a CA6 vaccine. This infection model provides a useful tool for future studies on vaccines or antiviral reagents against CA6.

Acknowledgments

This work was supported by a grant from the National Natural Science Foundation of China [grant numbers 31670933]; the Technological Innovation Platform Foundation of Fujian Province [grant number 2014Y2004]; the Natural Science Foundation of Fujian Province [grant number 2015J05073]; and the Technological Platform Foundation of Xiamen [grant number 350205Z20154007]. The funders had no role in the study design, data collection and analysis, decision to publish, or preparation of the manuscript.

References

- Bian, L., Wang, Y., Yao, X., Mao, Q., Xu, M., Liang, Z., 2015. Coxsackievirus A6: a new emerging pathogen causing hand, foot and mouth disease outbreaks worldwide. *Expert Rev. anti-infective Ther.* 13, 1061–1071.
- Cabrerizo, M., Tarrago, D., Munoz-Almagro, C., Del Amo, E., Dominguez-Gil, M., Eiros, J.M., Lopez-Miragaya, I., Perez, C., Reina, J., Otero, A., Gonzalez, I., Echevarria, J.E., Trallero, G., 2014. Molecular epidemiology of enterovirus 71, coxsackievirus A16 and A6 associated with hand, foot and mouth disease in Spain. *Clin. Microbiol. Infect.* 20, 0150–0156 the official publication of the European Society of Clinical Microbiology and Infectious Diseases.
- Caine, E.A., Fuchs, J., Das, S.C., Partidos, C.D., Osorio, J.E., 2015. Efficacy of a trivalent hand, foot, and mouth disease vaccine against enterovirus 71 and coxsackieviruses A16 and A6 in mice. *Viruses* 7, 5919–5932.
- Centers for Disease Control and Prevention, 2012. Notes from the field: severe hand, foot, and mouth disease associated with coxsackievirus A6—Alabama, Connecticut, California, and Nevada, November 2011–February 2012. *MMWR. Morb. Mortal. Wkly. Rep.* 61, 213–214.
- Christoffers, W.A., Riezebos-Brilman, A., Kardaun, S.H., 2016. Atypical presentation of painful vesicles on the hands and feet in an immunocompromised adult. *J. Clin. virol.* 78, 129–131 the official publication of the Pan American Society for Clinical Virology.
- Downing, C., Ramirez-Fort, M.K., Doan, H.Q., Benoist, F., Oberste, M.S., Khan, F., Tyring, S.K., 2014. Coxsackievirus A6 associated hand, foot and mouth disease in adults: clinical presentation and review of the literature. *J. Clin. virol.* 60, 381–386 the official publication of the Pan American Society for Clinical Virology.
- Feder Jr., H.M., Bennett, N., Modlin, J.F., 2014. Atypical hand, foot, and mouth disease: a vesiculobullous eruption caused by Coxsackie virus A6. *Lancet Infect. Dis.* 14, 83–86.
- Fonseca, M.C., Sarmiento, L., Resik, S., Martinez, Y., Hung, L.H., Morier, L., Pinon, A., Valdez, O., Kouri, V., Gonzalez, G., 2014. Coxsackievirus A6 and enterovirus 71 causing hand, foot and mouth disease in Cuba, 2011–2013. *Arch. Virol.* 159, 2451–2455.
- Gifford, R., Dalldorf, G., 1951. The morbid anatomy of experimental Coxsackie virus infection. *Am. J. Pathol.* 27, 1047–1063.
- Gopalkrishna, V., Patil, P.R., Patil, G.P., Chitambar, S.D., 2012. Circulation of multiple enterovirus serotypes causing hand, foot and mouth disease in India. *J. Med. Microbiol.* 61, 420–425.
- Han, J.F., Xu, S., Zhang, Y., Zhu, S.Y., Wu, D.L., Yang, X.D., Liu, H., Sun, B.X., Wu, X.Y., Qin, C.F., 2014. Hand, foot, and mouth disease outbreak caused by coxsackievirus A6, China, 2013. *J. Infect.* 69, 303–305.
- Keller, M.A., Stiehm, E.R., 2000. Passive immunity in prevention and treatment of infectious diseases. *Clin. Microbiol. Rev.* 13, 602–614.
- Klein, M., Chong, P., 2015. Is a multivalent hand, foot, and mouth disease vaccine feasible? *Hum. Vaccines Immunother.* 11, 2688–2704.
- Kobayashi, M., Makino, T., Hanaoka, N., Shimizu, H., Enomoto, M., Okabe, N., Kanou, K., Konagaya, M., Oishi, K., Fujimoto, T., 2013. Clinical manifestations of coxsackievirus A6 infection associated with a major outbreak of hand, foot, and mouth disease in Japan. *Jpn. J. Infect. Dis.* 66, 260–261.
- Lei, X., Cui, S., Zhao, Z., Wang, J., 2015. Etiology, pathogenesis, antivirals and vaccines of hand, foot, and mouth disease. *Natl. Sci. Rev.* 2, 268–284.
- Li, Z., Xu, L., He, D., Yang, L., Liu, C., Chen, Y., Shih, J.W., Zhang, J., Zhao, Q., Cheng, T., Xia, N., 2014. In vivo time-related evaluation of a therapeutic neutralization monoclonal antibody against lethal enterovirus 71 infection in a mouse model. *PLoS One* 9, e109391.
- Liu, C.C., Chow, Y.H., Chong, P., Klein, M., 2014. Prospect and challenges for the development of multivalent vaccines against hand, foot and mouth diseases. *Vaccine* 32, 6177–6182.
- Liu, C.C., Guo, M.S., Wu, S.R., Lin, H.Y., Yang, Y.T., Liu, W.C., Chow, Y.H., Shieh, D.B., Wang, J.R., Chong, P., 2016. Immunological and biochemical characterizations of coxsackievirus A6 and A10 viral particles. *Antivir. Res.* 129, 58–66.
- Liu, Q., Tong, X., Huang, Z., 2015. Towards broadly protective polyvalent vaccines against hand, foot and mouth disease. *Microbes Infect./Inst. Pasteur* 17, 155–162.
- Mao, Q., Wang, Y., Gao, R., Shao, J., Yao, X., Lang, S., Wang, C., Mao, P., Liang, Z., Wang, J., 2012. A neonatal mouse model of coxsackievirus A16 for vaccine evaluation. *J. Virol.* 86, 11967–11976.
- Mao, Q., Wang, Y., Yao, X., Bian, L., Wu, X., Xu, M., Liang, Z., 2014. Coxsackievirus A16: epidemiology, diagnosis, and vaccine. *Hum. Vaccines Immunother.* 10, 360–367.
- Mao, Q.Y., Wang, Y., Bian, L., Xu, M., Liang, Z., 2016. EV71 vaccine, a new tool to control outbreaks of hand, foot and mouth disease (HFMD). *Expert Rev. Vaccines* 1–8.
- Mirand, A., Henquell, C., Archimbaud, C., Ughetto, S., Antona, D., Bailly, J.L., Peigue-Lafeuille, H., 2012. Outbreak of hand, foot and mouth disease/herpangina associated with coxsackievirus A6 and A10 infections in 2010, France: a large citywide, prospective observational study. *Clin. Microbiol. Infect.* 18, E110–E118 the official publication of the European Society of Clinical Microbiology and Infectious Diseases.
- Miyamoto, A., Hirata, R., Ishimoto, K., Hisatomi, M., Wasada, R., Akita, Y., Ishihara, T., Fujimoto, T., Eshima, N., Hatano, Y., Katagiri, K., Fujiwara, S., 2014. An outbreak of hand-foot-and-mouth disease mimicking chicken pox, with a frequent association of onychomadesis in Japan in 2009: a new phenotype caused by coxsackievirus A6. *Eur. J. Dermatol. EJD* 24, 103–104.
- Montes, M., Artieda, J., Pineiro, L.D., Gastesi, M., Diez-Nieves, I., Cilla, G., 2013. Hand, foot, and mouth disease outbreak and coxsackievirus A6, northern Spain, 2011. *Emerg. Infect. Dis.* 19.
- Muehlenbachs, A., Bhatnagar, J., Zaki, S.R., 2015. Tissue tropism, pathology and pathogenesis of enterovirus infection. *J. Pathol.* 235, 217–228.
- Osterback, R., Vuorinen, T., Linna, M., Susi, P., Hyyppia, T., Waris, M., 2009. Coxsackievirus A6 and hand, foot, and mouth disease, Finland. *Emerg. Infect. Dis.* 15, 1485–1488.
- Reed, L.J., Muench, H., 1938. A simple method of estimating fifty per cent endpoints. *Am. J. Epidemiol.* 27, 493–497.
- Reina, J., Penaranda, M., Cabrerizo, M., 2014. Eczema coxsackium (Coxsackievirus A6) in an human immunodeficiency virus infected adult patient. *Rev. Clin. espanola* 214, 228–229.
- Schmidt, N.J., Ho, H.H., Lennette, E.H., 1975. Propagation and isolation of group A coxsackieviruses in RD cells. *J. Clin. Microbiol.* 2, 183–185.
- Seki, Y., Makino, T., Mizawa, M., Hamashima, T., Sasahara, M., Shimizu, T., 2014. Immunohistological examination of a skin lesion in a Japanese case with hand, foot and mouth disease caused by coxsackie-virus A6. *Eur. J. dermatol. EJD* 24, 506–507.
- Stewart, C.L., Chu, E.Y., Introcaso, C.E., Schaffer, A., James, W.D., 2013. Coxsackievirus A6-induced hand-foot-mouth disease. *JAMA Dermatol.* 149, 1419–1421.
- Wang, Y.F., Yu, C.K., 2014. Animal models of enterovirus 71 infection: applications and limitations. *J. Biomed. Sci.* 21, 31.
- Wei, S.H., Huang, Y.P., Liu, M.C., Tsou, T.P., Lin, H.C., Lin, T.L., Tsai, C.Y., Chao, Y.N., Chang, L.Y., Hsu, C.M., 2011. An outbreak of coxsackievirus A6 hand, foot, and mouth disease associated with onychomadesis in Taiwan, 2010. *BMC Infect. Dis.* 11, 346.
- Wu, Y., Yeo, A., Phoon, M.C., Tan, E.L., Poh, C.L., Quak, S.H., Chow, V.T., 2010. The largest outbreak of hand; foot and mouth disease in Singapore in 2008: the role of enterovirus 71 and coxsackievirus A strains. *Int. J. Infect. Dis. IJID* 14, e1076–1081 official publication of the International Society for Infectious Diseases.
- Xing, W., Liao, Q., Viboud, C., Zhang, J., Sun, J., Wu, J.T., Chang, Z., Liu, F., Fang, V.J., Zheng, Y., 2014. Hand, foot, and mouth disease in China, 2008–12: an epidemiological study. *Lancet Infect. Dis.* 14, 308–318.
- Yang, L., He, D., Tang, M., Li, Z., Liu, C., Xu, L., Chen, Y., Du, H., Zhao, Q., Zhang, J., Cheng, T., Xia, N., 2014. Development of an enzyme-linked immunosorbent spot assay to measure serum-neutralizing antibodies against coxsackievirus B3. *Clin. Vaccine Immunol.* CVI 21, 312–320.
- Yang, L., Li, S., Liu, Y., Hou, W., Lin, Q., Zhao, H., Xu, L., He, D., Ye, X., Zhu, H., Cheng, T., Xia, N., 2015. Construction and characterization of an infectious clone of coxsackievirus A6 that showed high virulence in neonatal mice. *Virus Res.* 210, 165–168.
- Ye, X., Yang, L., Jia, J., Han, J., Li, S., Liu, Y., Xu, L., Zhao, H., Chen, Y., Li, Y., Cheng, T., Xia, N., 2016. Development of sandwich ELISAs that can distinguish different types of coxsackievirus A16 viral particles. *Appl. Microbiol. Biotechnol.* 100, 2809–2815.